• Masses can be inferred from binary orbit observations. For example, **astrometric masses** can be discerned from the $m_1/m_2 = a_2/a_1$ orbit ratio and knowledge of the mass of the main sequence companion. Usually, radii can be inferred from the Stefan-Boltzmann law, though light curves can present analternative if there is orbital occultation. For either, M/R can be checked against **spectral gravitational redshifts**.

∗ Field white dwarfs lack binary mass constraints, and so often astronomers resort to detailed models of hydrogen+helium atmospheres and their predictions of line shape and broadening to measure the **surface gravity** $g = GM/R^2$. With R obtained from the S-B law, this gives a mass estimate.

• Observational $M - R$ constraints have not yet reached a stasis, though there is approximate consensus for select nearby white dwarfs such as 40 Eridani B, Sirius B, Procyon B and Stein 2051 B, all being visual binaries.

Table 1: Mass/Radius Determination for Nearby White Dwarfs in Binaries

White Dwarf	Astrometric Mass ($M_\odot$)	Radius ($R_\odot/100$)	$v_g = GM/Rc$ (km sec^{-1})^c	Redshift^d (km sec^{-1})
Sirius B ^{a}	1.000 ± 0.016	0.84 ± 0.02	75.7 ± 3.0	80.4 ± 40.8
40 Eridani B ^{a}	0.50 ± 0.02	1.36 ± 0.02	23.4 ± 1.3	26.5 ± 1.5
Procyon B ^{a}	0.60 ± 0.03	0.96 ± 0.04	39.8 ± 3.6	–
Stein 2051 B ^{b}	0.675 ± 0.051	1.14 ± 0.04	37.7 ± 4.2	–

Notes: ^{a}Provencal et al. (1998, *ApJ*) for Sirius B, 40 Eri B & Procyon B. ^{b}Sahu et al. (2017, *Science*) for Stein 2051 B and astrometric microlensing. ^{c}The gravitational redshift formula is $v_g = 0.636(M/M_\odot)\,(R_\odot/R)$ km/sec. ^{d}The Doppler redshift for Sirius B is from Barstow et al. (2005, MNRAS), for 40 Eridani B from Koester & Weidemann (1991, AJ).

• Clever approaches are available in select examples, such as the astrometric microlensing mass determination of Stein 2051 B by Sahu et al. (2017). This takes advantage of the superb angular resolution of Hubble STIS.

$\boxed{\textbf{Plot:}}$ Microlensing determinations of Mass of Stein 2051 B

Microlensing and Mass of WD Stein 2051 B

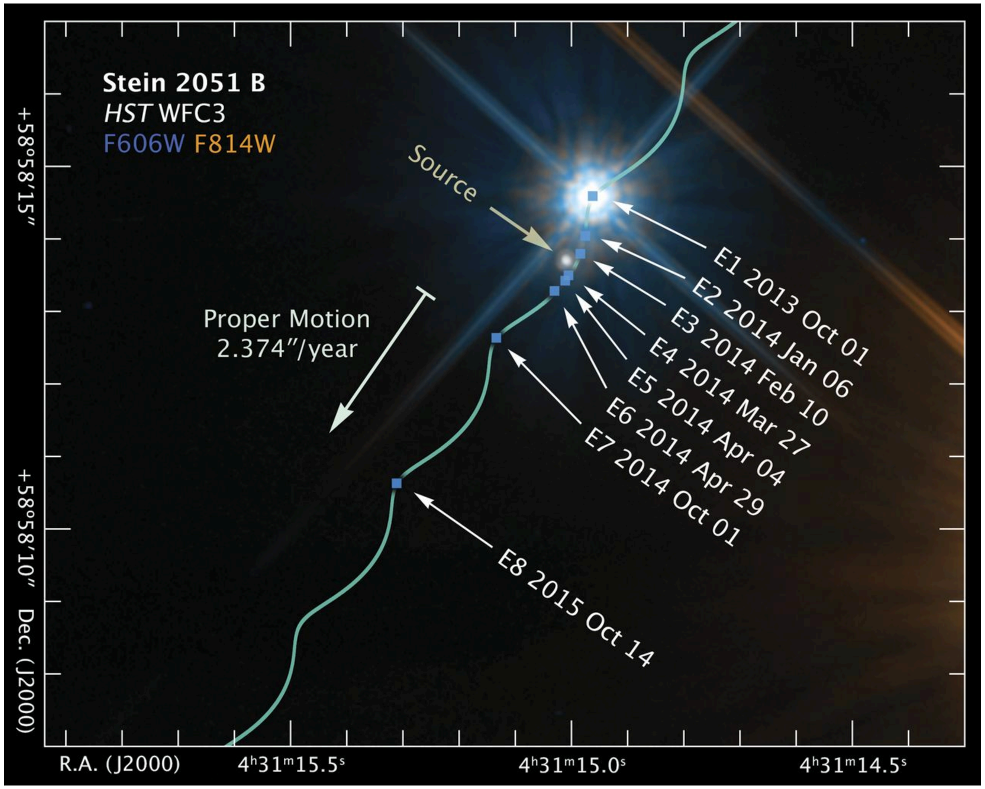

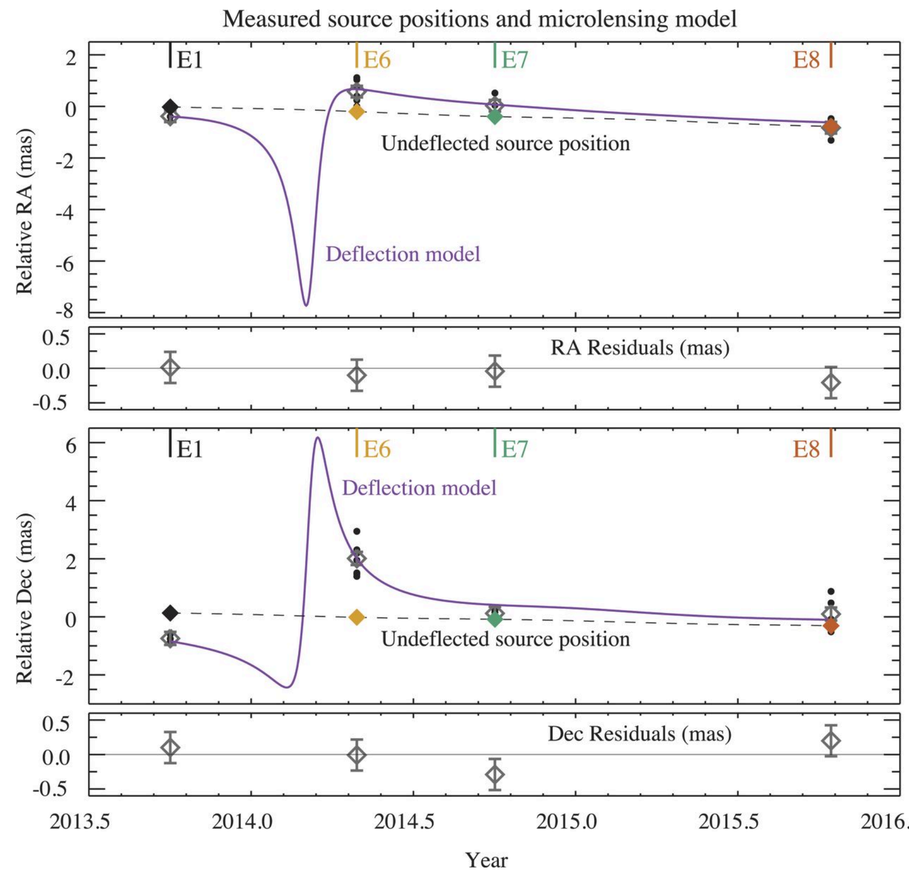

- Hubble observations: General relativistic astrometric microlensing wobble of background star (source) on the scale of ~2 mas, due to passage of Stein 2051 B leads to a mass measurement of $0.675 \pm 0.051 M_\odot$ for this white dwarf.
  - Stein 2051 B proper motion wobble is due to Earth orbit parallax.
- K. Sahu et al., *Science* **356**, 1046 (2017).

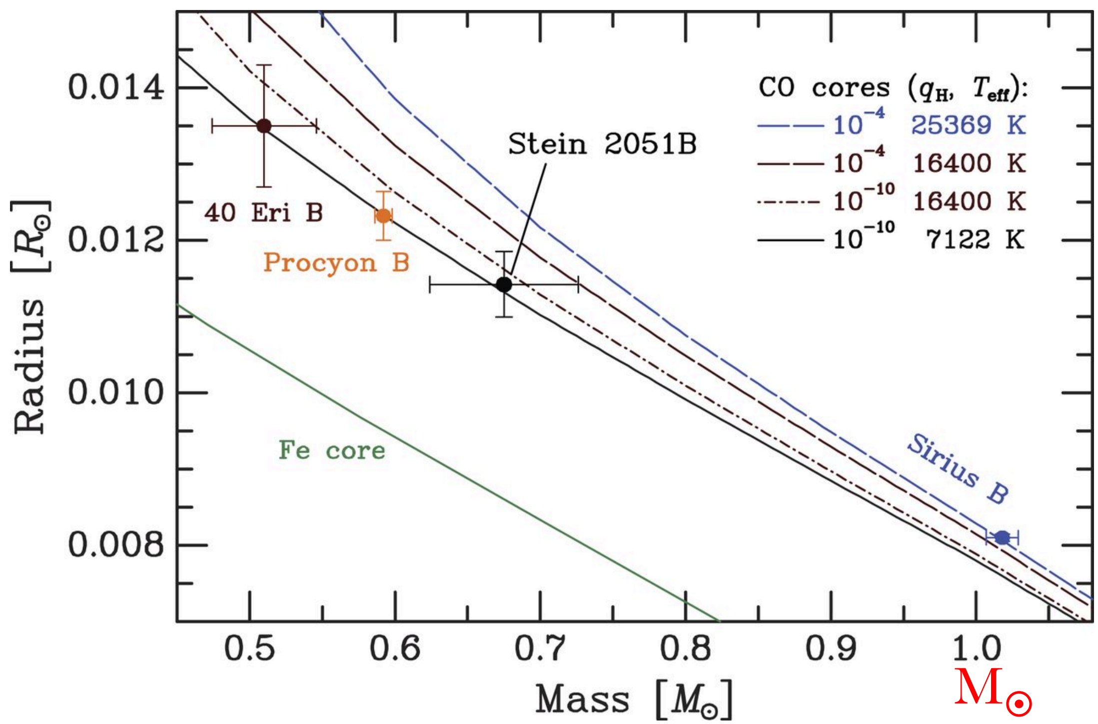

White Dwarf Mass-Radius Relation

- Sahu et al.
  (Science **356**, 1046, 2017)

Table 1: Mass/Radius Determination for Nearby White Dwarfs in Binaries

White Dwarf	Astrometric Mass ($M_\odot$)	Radius ($R_\odot/100$)	$v_g = GM/Rc$ (km sec^{-1})[c]	Redshift[d] (km sec^{-1})
Sirius B [a]	1.000 ± 0.016	0.84 ± 0.02	75.7 ± 3.0	80.4 ± 40.8
40 Eridani B [a]	0.50 ± 0.02	1.36 ± 0.02	23.4 ± 1.3	26.5 ± 1.5
Procyon B [a]	0.60 ± 0.03	0.96 ± 0.04	39.8 ± 3.6	–
Stein 2051 B [b]	0.675 ± 0.051	1.14 ± 0.04	37.7 ± 4.2	–

Notes: [a]Provencal et al. (1998, *ApJ*) for Sirius B, 40 Eri B & Procyon B.
[b]Sahu et al. (2017, *Science*) for Stein 2051 B and astrometric microlensing.
[c]The gravitational redshift formula is $v_g = 0.636(M/M_\odot)(R_\odot/R)$ km/sec.
[d]The Doppler redshift for Sirius B is from Barstow et al. (2005, MNRAS), for 40 Eridani B from Koester & Weidemann (1991, AJ).

1.3 The Chandrasekhar Mass Limit

• For the non-relativistic mass-radius relations, in principle the star can be infinitely massive and arbitrarily small. What happens as $M_{\rm wd}$ increases?

• Relativistic effects limit the mass a white dwarf can possess. The equation of state $P \propto n_e^{5/3}$ in Eq. (7) is no longer viable. We can use the pressure integral to determine that $P = n_e pv/3$ for $v \leq c$. Asserting that $\Delta x \sim n_e^{-1/3}$, we can use Heisenberg's uncertainty principle to establish

$$p \sim \frac{\hbar}{\Delta x} \approx \hbar n_e^{1/3} \quad . \tag{10}$$

This can be arbitrarily high. The deduced non-relativistic speed would be $v = p/m_e \approx \hbar n_e^{1/3}/m_e$, leading to the equation of state in Eq. (7).

• When the electron density exceeds around $(m_e c/\hbar)^3$ (the inverse of the cube of the Compton wavelength), the degenerate electrons are relativistic, and we set $v \sim c$. It then follows that

$$P = \frac{1}{3} n_e pc = \frac{(3\pi^2)^{1/3}}{4} \hbar c \, n_e^{4/3} \quad , \tag{11}$$

a truly relativistic equation of state. For $\mu_e = A/Z$ as the **mean molecular weight** of the electron, we can write this in **polytropic form**:

$$P = \mathcal{K} \rho^{\Gamma} \quad , \quad \mathcal{K} = \frac{(3\pi^2)^{1/3}}{4} \frac{\hbar c}{(\mu_e m_p)^{4/3}} \quad , \tag{12}$$

with $\Gamma = 4/3$. $\mathcal{K}$ is now specified, but only for the relativistic case $n_e \gtrsim \lambda\!\!\!^{-}_{\rm C}{}^{-3}$. We can ascertain the general pressure scale, noting that for hydrogen, $\rho \sim 10^6 \,\mathrm{g\, cm^{-3}}$ gives $n_e \sim 6 \times 10^{29} \,\mathrm{cm}^3$. Accordingly,

$$P = \frac{1.23 \times 10^{23}}{\mu_e^{4/3}} \left(\frac{\rho}{10^6 \,\mathrm{g\, cm^{-3}}} \right)^{4/3} \mathrm{dyne\, cm^{-2}} \quad . \tag{13}$$

This is a bit lower than the scale for the non-relativistic degenerate electron gas, implying that the relativistic EOS only arises in white dwarfs at densities a fair bit higher than $\rho \sim 10^6 \,\mathrm{g\, cm^{-3}}$, i.e. generally in the stellar interior.

The gravitational pressure GM^2/R^4 in Eq. (1) intrinsically scales as $M^{2/3}\, n_e^{4/3}$ also (since $R \propto (M/\rho)^{1/3}$). Hence balance can only be achieved if the degeneracy pressure is sufficiently great, or equivalently if the white dwarf mass is sufficiently small. This leads to

$$\boxed{M_{\rm wd} \;\lesssim\; M_{\rm Ch} \;\sim\; \left(\frac{Z}{Am_p}\right)^2 \left(\frac{\hbar c}{G}\right)^{3/2} \quad ,} \tag{14}$$

or an exact result of $M_{\rm Ch} = 1.44 M_{\odot}$. This is the famous **Chandrasekhar mass limit** of white dwarfs, discovered by Chandrasekhar in 1931. It assumes $Z/A = 0.5$ for C+O, and is independent of the electron mass.

Plot: White Dwarf Mass and Radius Dependence on Density

∗ Note that $(\hbar c/G)^{1/2} \approx 2.18 \times 10^{-5}\,$g is the **Planck mass**.

• This fundamental mass can be increased somewhat by permitting the star to rotate as a Maclaurin spheroid: angular momentum provides additional support against the pull of gravity.

Plot: Rotational Increase of White Dwarf Mass Limit

• Note also that magnetic fields can increase the buoyancy of outer layers of white dwarfs by a few percent, although not leading to appreciable increases in masses. WD fields can be measured via the Zeeman effect on hydrogen line splitting and also frequency shift (when $B \gtrsim 1\,$MGauss).

∗ Observations of this are easiest in white dwarfs of stronger magnetization, leading to a population range of $10^4 \lesssim B \lesssim 10^9\,$Gauss for 600 WDs in the Sloan Digital Sky Survey (SDSS). The highest of these are larger than flux freezing arguments indicate, suggesting that some dynamo action is at play during formation.

Plot: White Dwarf Magnetic Fields

White dwarf mass and radius dependence on mass density ρ_c

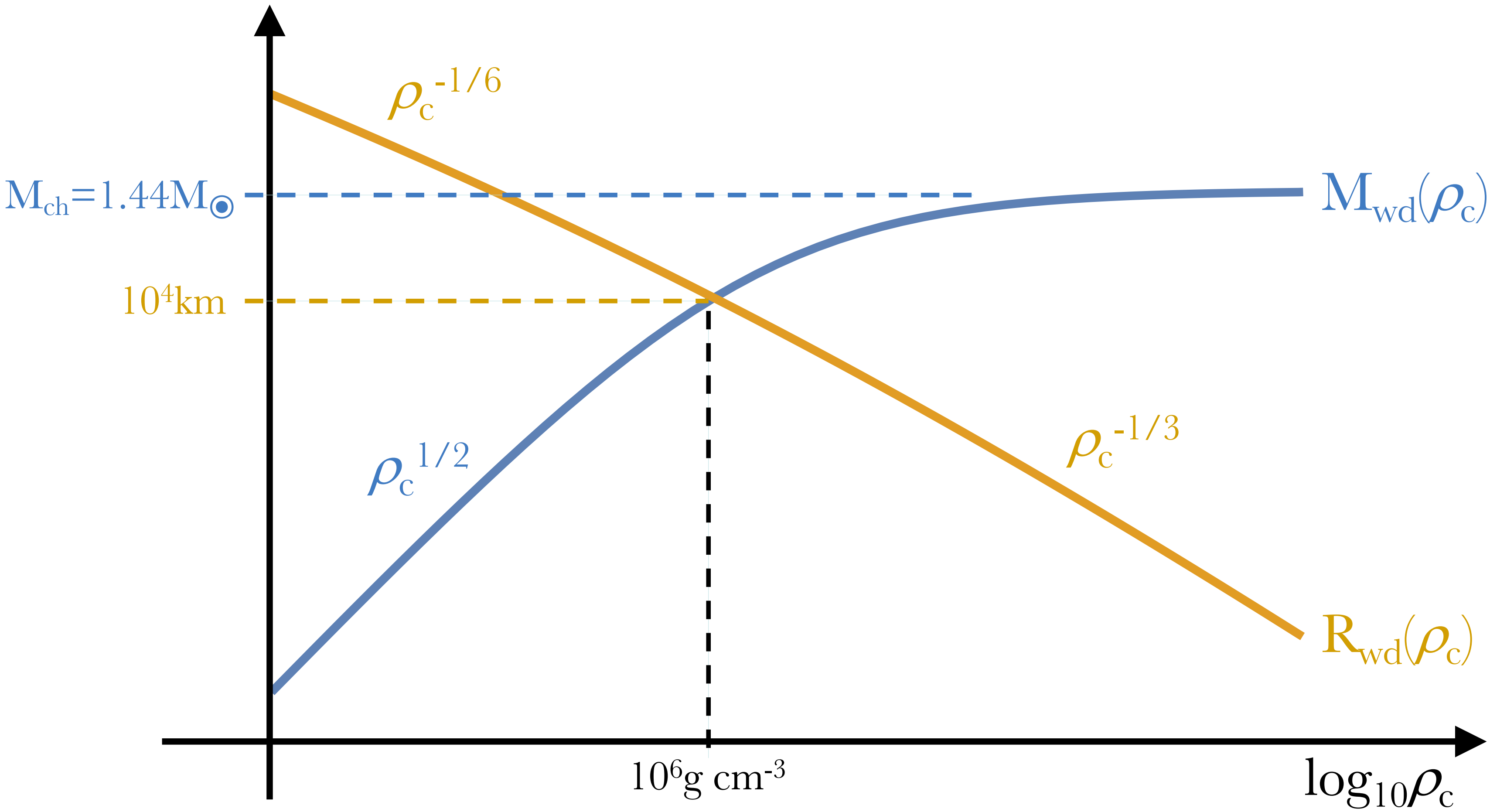

- Dependence of stellar mass M and radius R on central density ρ_c.

Rotational increase of White Dwarf Mass beyond the Chandrasekhar Limit

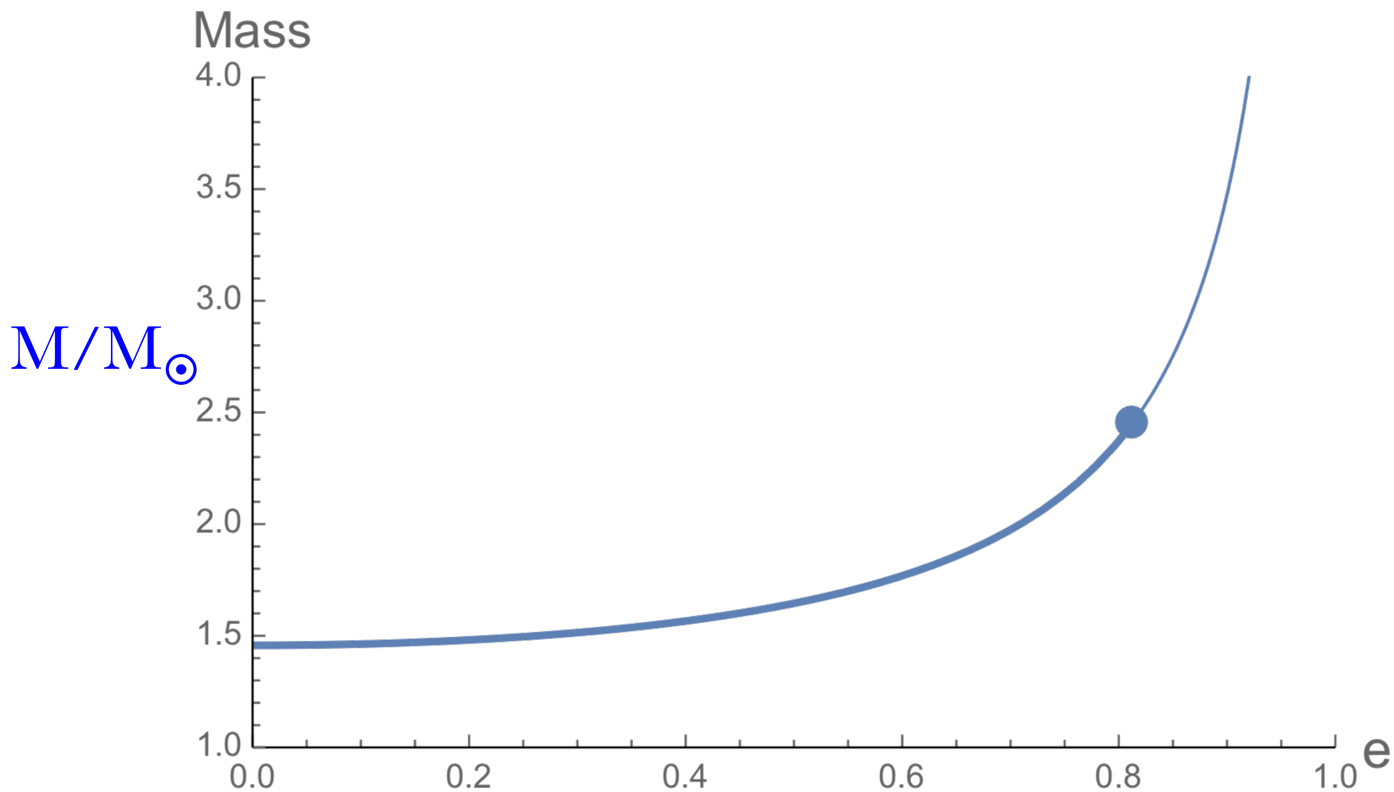

- Mass increase of Chandrasekhar white dwarfs that are Maclaurin spheroids of oblateness eccentricity e, that is uniquely coupled to the rotation parameter $\Omega/[2\pi G\rho]^{1/2}$.
- Only eccentricities less than $e=0.8216$ (blue dot) are secularly stable (heavy curve), and this ultimately limits the mass enhancement to $2.45M_\odot$ for a C/O white dwarf.

White Dwarf Magnetic Fields

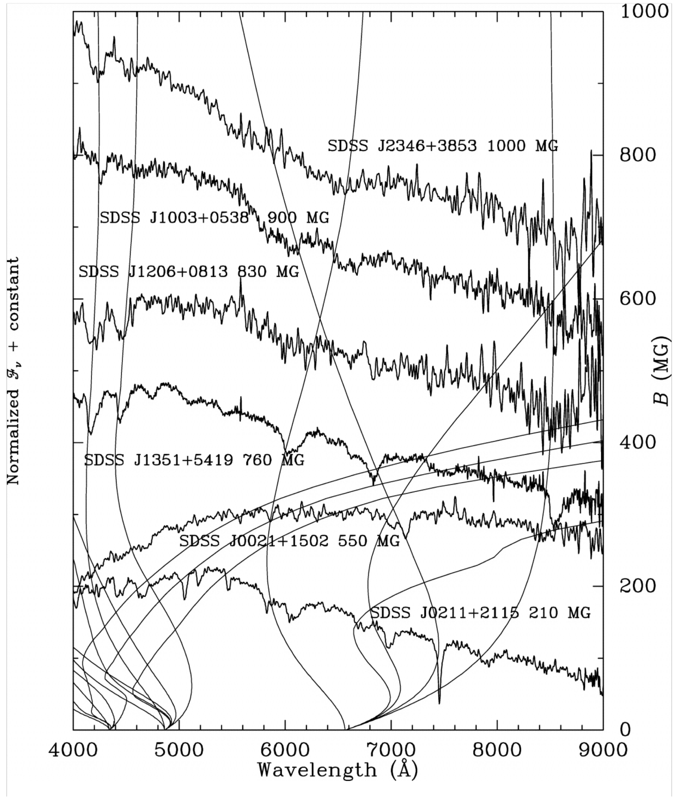

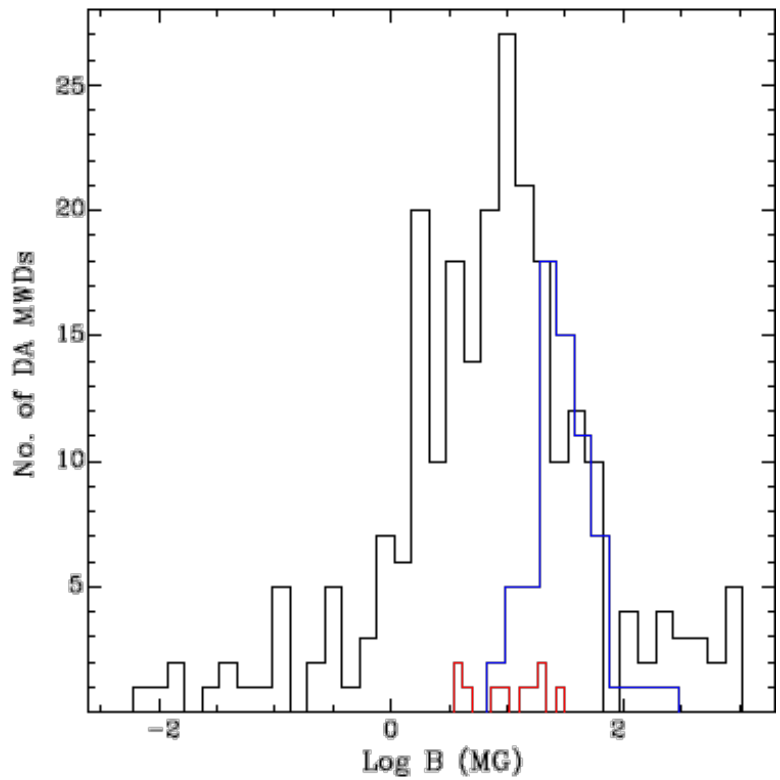

- *Left panel*: Optical spectra for six WDs with Hα and Hβ lines split by the Zeeman effect, which is used to measure B. Curves are wavelength variations of split lines as a function of field strength (right axis). Fig. 1 from Vanlandingham et al. (2005, AJ **130**, 734).
- *Right panel*: Magnetic field distribution of ~600 magnetic white dwarfs in the Sloan Digital Sky Survey (SDSS). Black histogram is for isolated WDs, and blue is for polars. Fig. 8 from Ferrario, de Martino & Gaensicke (2015, SSRv **191**, 111).

2 White Dwarf Cooling

Because there is no thermonuclear burning in their interiors, white dwarfs essentially cool via surface thermal radiation without altering their radius; the hydrostatic balance is not altered during their luminous lifetimes. **C & O, Sec. 16.5**

$\ast$ However, there is slow **pyconuclear burning** due to quantum tunneling through the Coulomb barrier because of the zero-point Fermi energy ε_F .

• In the layers below the *nondegenerate* photosphere, heat is transported by **electron conduction**, since such conductivity is high when the electrons are degenerate. The efficiency of this is high, so that the stellar interior is *effectively isothermal.* [`Sketch this.`]

• Convection is not important in white dwarfs. Hence the radiative transfer equation describing photon diffusion is operable, so that the luminosity couples to the opacity κ :

$$L \; = \; -\frac{4\pi r^2 c}{3\kappa\rho}\, \frac{d}{dr}(aT^4) \quad . \tag{15}$$

The radial gradient of the blackbody flux is small and approximately constant. **Kramer's opacity**, similar to the Rosseland mean, scales as $\kappa \propto T^{-3.5}$ in the operable temperature range (i.e., PE effect). Hence

$$L \; \propto \; \frac{1}{\kappa} \; \propto \; T^{7/2} \quad . \tag{16}$$

Detailed derivations of the equation of state and the hydrostatic balance in the surface layers yields a white dwarf luminosity of

$$L_{wd} \; \sim \; C\, T_c^{7/2} \quad , \quad C \; = \; 7.3 \times 10^5 \left(\frac{M_{wd}}{M_\odot} \right) \frac{\mu}{Z} \quad . \tag{17}$$

Here C has units of erg sec^{-1} K$^{-7/2}$. Since the thermal energy of the stellar interior is

$$U \; = \; \frac{M_{wd}}{Am_H}\, \frac{3}{2}\, kT_c \quad , \tag{18}$$

then a rough estimate of the cooling timescale (the high conductivity redistributes the thermal energy rapidly through the star) is

$$\tau_c \sim \frac{U}{L_{wd}} = \frac{3\,M_{wd}k}{2Am_H C T_c^{5/2}} \quad . \tag{19}$$

Note that since $C \propto M_{wd}$, this timescale is roughly independent of the white dwarf mass!

• Solving the cooling equation $-dU/dt = L_{wd}$ then gives

$$T_c(t) = \frac{T_0}{(1+t/\tau_0)^{2/5}} \quad , \quad L_{wd}(t) = \frac{L_0}{(1+t/\tau_0)^{7/5}} \quad , \tag{20}$$

where

$$\tau_0 = \frac{3\,M_{wd}k}{5Am_H C T_0^{5/2}} \quad . \tag{21}$$

Furthermore, since all white dwarfs start with similar central temperatures, this cooling curve is more or less a standard "decay," with $\tau_0 \sim 1.5\times 10^8$ years.

• Deviations from the standard cooling curve are expected, and are observed, at late stages of evolution (typically $\sim 5\times 10^9$ years) due to **crystallization**.

∗ Cooling lowers T_{wd} to the point where dense C and O form a lattice structure, from inside first, where P is high, to outside. This structure is like diamond formation under extreme pressure.

∗ Crystallization is a phase transition that *releases* latent heat – consequently slowing the cooling, and generating a "bump" in the cooling curve.

Plot: White Dwarf Specific Heat Capacity

• Robust cooling curve leads to usefulness of white dwarfs as age calibrators in the universe.

Plot: White Dwarf Luminosity Distribution

• The Milky Way white dwarf population suggests an age of $\gtrsim 9.0 \pm 1.8 \times 10^9$ years. To this must be added the contribution for main sequence evolution prior to the white dwarf phase.

Specific Heat Capacity: Debye Regime

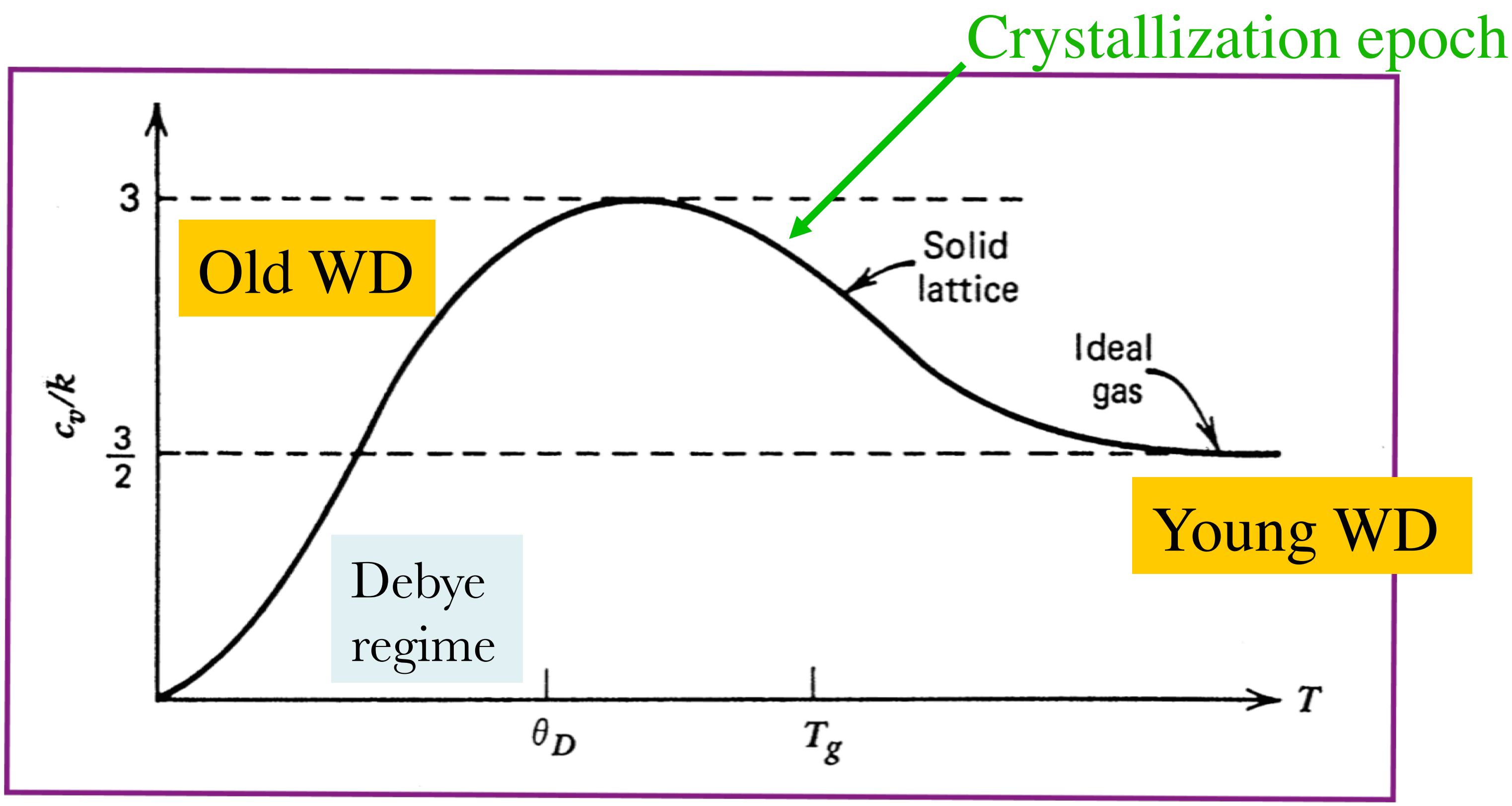

- Specific heat capacity as a function of temperature – schematic diagram <u>for ions only</u>. At high temperature, the lattice melts, forming an ideal gas with $c_V=3k/2$. At modest temperatures, crystallization results, and c_V increases to 3k. When $T < \Theta_D$, collective influences on vibrational modes (Debye screening) lower $c_V \propto T^3$.

White Dwarf Luminosity Function

(Isern, Artigas & García-Berro, EPJ 43, 05002, 2013)

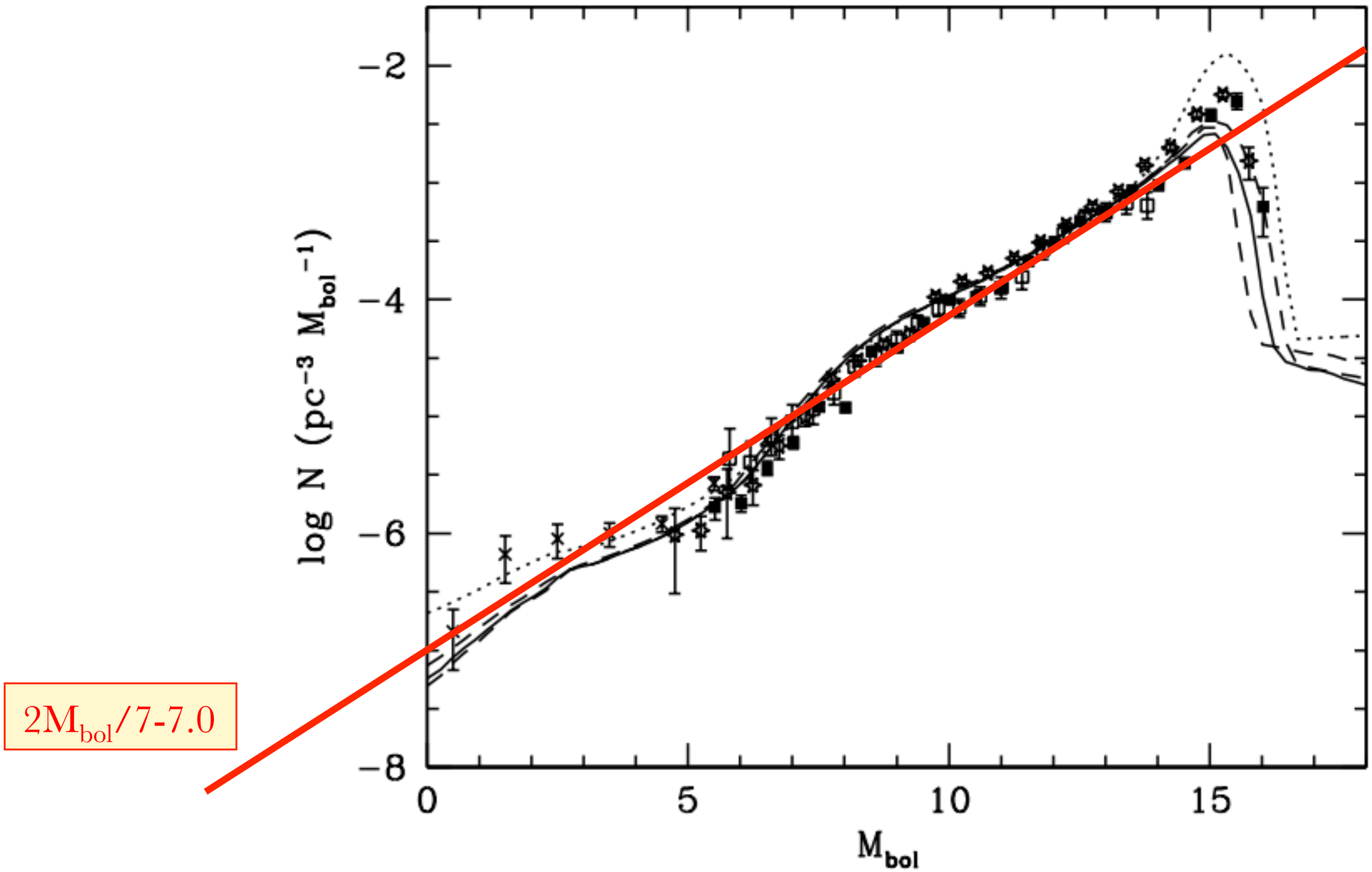

- Large survey data for the white dwarf luminosity function. Models for curves comprise different Galactic disk descriptions and star formation rates.